Radar Processing, Technology and Applications II, Proc. SPIE #3161, p. 126-136 (1997)

# Classification of Ships in Airborne SAR Imagery Using Backpropagation Neural Networks

Hossam Osman*, Li Pan†, Steven D. Blostein†, and Langis Gagnon‡

*Department of Computer and Systems Engineering
Ain Shams University
Abbasia, Cairo, Egypt, 11381

†Department of Electrical and Computer Engineering
Queen's University
Kingston, Ontario, Canada, K7L 3N6

‡R&D Department, Lockheed Martin Electronic Systems Canada
Montreal, Quebec, Canada, H4P 1K6

**Abstract**

This paper proposes using a backpropagation (BP) neural network for the classification of ship targets in airborne synthetic aperture radar (SAR) imagery. The ship targets consisted of 2 destroyers, 2 cruisers, 2 aircraft carriers a frigate and a supply ship. A SAR image simulator was employed to generate a training set, a validation set, and a test set for the BP classifier. The features required for classification were extracted from the SAR imagery using three different methods. The first method used a reduced resolution version of the whole SAR image as input to the BP classifier using simple averaging. The other two methods used the SAR image range profile either before or after a local-statistics noise filtering algorithm for speckle reduction. Performance on an extensive test set demonstrated the performance and computational advantages of applying the neural classification approach to targets in airborne SAR imagery. Improvements due to the use of multi-resolution features were also observed.

**Keywords:** SAR, pattern classification, feature extraction, backpropagation neural networks

# 1 INTRODUCTION

Synthetic aperture radar (SAR) is a microwave-based sensor that is characterized by the production of images of very high resolution and operates in all-weather conditions. As real-time airborne synthetic aperture radar (SAR) imagery comes into widespread use, there is interest in automated decision and control systems that rely on acquired on-board image data. Artificial neural networks have demonstrated success in a variety of applications. Characteristics such as intrinsic parallelism, fast classification time and no required prior statistical knowledge of the data have made the neural approach to pattern classification quite attractive. Automatic methods for the interpretation of SAR imagery containing ship patterns have been proposed in recent literature[1-6]. However, previous results in this area have either considered ship classification under simplifying assumptions[1] or have been concerned with ship detection rather than ship classification[2-6].

Here, this paper proposes using a back-propagation (BP) neural network to classify ship targets detected and segmented in airborne SAR imagery. Section 2 describes the generation of the SAR imagery needed to construct and test the BP network classifier. Section 3 discusses training and testing the classifier and presents the experimental results. Finally, Section 4 summarizes the main conclusions of this investigation.

# 2 SAR IMAGERY GENERATION

A data set of 8 ship classes was generated using a SAR image simulator[7]. It was assumed that the images were corrected for motion effects but contained speckle[8]. The classes represented 2 types of destroyers, 2 cruisers, 2 aircraft carriers, a frigate and a supply ship. The class number assigned to each class type is given in Table 1. Since a ship signature depends on the ship orientation relative to the SAR sensor, a set of different aspect angles were generated in increments of $2^\circ$ until the whole range of interest was covered. Each collected signature was centered in a window of $80 \times 80$ pixels and scaled such that its minimum and maximum intensities corresponded to gray values of 0 and 255, respectively. For each ship class, at each aspect angle, eighteen $80 \times 80$ images with resolution 3 m $\times$ 3 m per pixel were generated. This yielded 864 images per class for a total of $8 \times 864 = 6912$ images. Sample SAR images are shown in Figure 1.

The generated images were divided into a training set, a validation set and a test set. The training and validation sets were needed to construct the BP classifier, whereas the test set was needed to

Figure 1: Sample SAR images. Each row contains images of one ship class obtained at different aspect angles.

| Class | Class Type |
|---|---|
| 1 | Destroyer |
| 2 | Cruiser |
| 3 | Destroyer |
| 4 | Supply ship |
| 5 | Aircraft carrier |
| 6 | Cruiser |
| 7 | Aircraft carrier |
| 8 | Frigate |

Table 1: Classes of the generated SAR data set.

measure classification performance. The division of the generated images was done such that for each ship class, at each aspect angle, six of the eighteen generated images were taken for the training set, six were taken for the validation set and six were taken for the test set. This resulted in 288 images per class per set for a total of $8 \times 288 = 2304$ images per set. In what follows, the usage of a BP network to classify ship patterns found in SAR images is described.

# 3 BACKPROPAGATION NETWORK CLASSIFIER

A 3-layer BP network classifier with 8 output units, where 8 is the number of ship classes, was employed. The number of network input units was set to the number of features extracted from a given SAR image. Three different algorithms of feature extraction were applied and compared. The first, denoted by Algorithm A, took the whole SAR image as an input to the BP classifier after using simple averaging to reduce its resolution to $16 \times 16$ input blocks. Thus, for Algorithm A, the BP network had 256 input units. Reduction of image resolution was done for computational purposes and to smooth, to some extent, the speckle present in the SAR images. The second algorithm, denoted by Algorithm B, took as an input the 80-pixel range profile of the SAR image, and the BP network had 80 input units. The range profile of one of the two aircraft carriers is shown in Figure 2. The third algorithm, denoted by Algorithm C, also took as an input the range profile of the SAR image, but after the application of a local-statistics noise filtering algorithm for speckle reduction[8]. The result of applying this noise filtering algorithm to the sample SAR images of Figure 1 is shown in Figure 3.

The number of the BP network hidden units was varied between 4 and 25 by increments of 3 units. For each number of hidden units, the network was trained by iteration through the available training set until convergence. In training the $j$th network output, the desired value was 1 if the

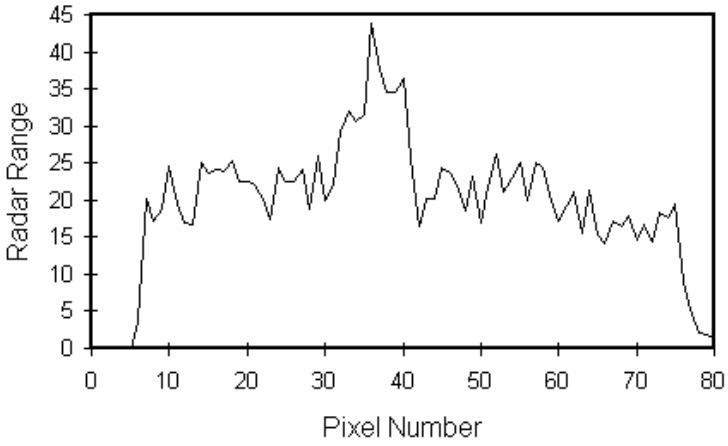


Figure 2: Range profile of an aircraft carrier.

given input belonged to the $j$th ship class, and was 0, otherwise. Using different network weight initializations, 10 training runs were performed. Once a training run was complete, the network classification performance on the already-prepared validation set was determined. Among the 10 classification values obtained for each number of hidden units for each of the three feature extraction algorithms, the best one was selected for comparison. The obtained results are plotted in Figure 4. As shown, for all three algorithms, the network classification performance on the validation set was maximized at 19 hidden units. Using 19 hidden units, the performance of the BP network on the test set was evaluated. Table 2 gives the correct classification rates, whereas Tables 3-5 give the confusion matrices for all three feature extraction algorithms. As reported, the BP classifier gave a correct classification rate as high as 98% on the 2304 SAR test set images. Due, in part, to the larger number of input features involved, Algorithm A significantly outperformed Algorithms B and C. As a result of speckle reduction, the performance of Algorithm C was better than that of Algorithm B. However, the improvement in performance was not that significant and for some ship classes Algorithm B gave a better performance.

| BP Algorithm | Classification |
|---|---|
| A (pixel block) | 0.983 |
| B (range profile) | 0.898 |
| C (pre-filtered range profile) | 0.918 |

Table 2: Correct classification rate on the test set.

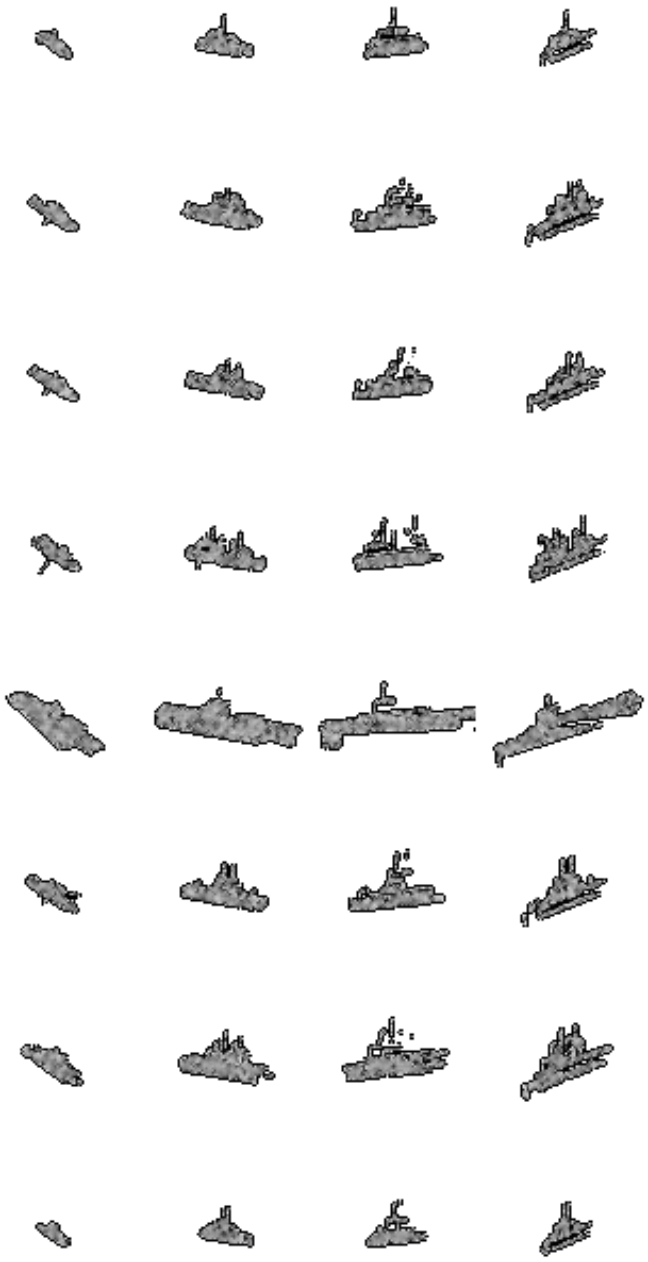

Figure 3: The sample SAR images of Figure 1 after applying a local-statistics speckle reduction algorithm. Each row contains images of one ship class obtained at different aspect angles.

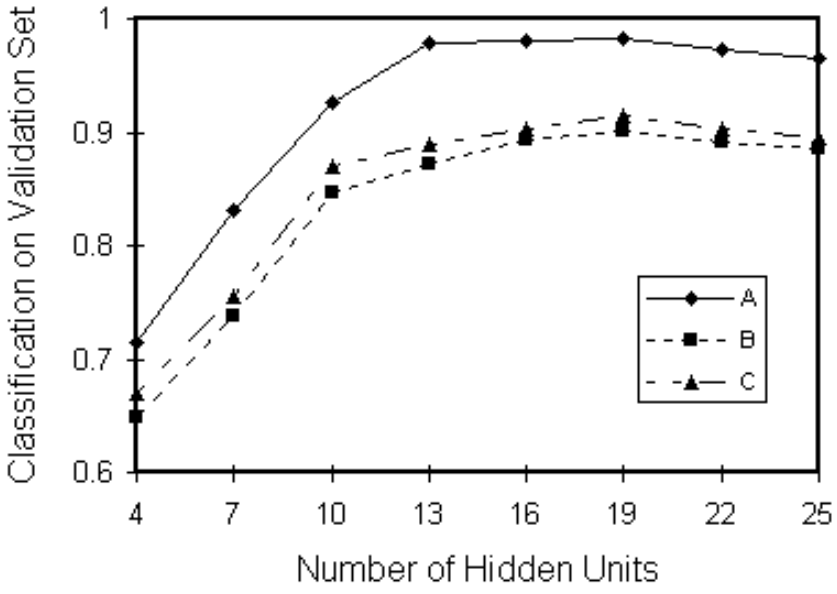


Figure 4: Correct classification rate on the validation set versus the number of hidden units for feature extraction algorithms A, B, and C.

| | Given Class | | | | | | | |
|---|---|---|---|---|---|---|---|---|
| | 1 | 2 | 3 | 4 | 5 | 6 | 7 | 8 |
| Desired Class | | | | | | | | |
| 1 | 277 | 0 | 0 | 0 | 0 | 0 | 0 | 11 |
| 2 | 0 | 274 | 14 | 0 | 0 | 0 | 0 | 0 |
| 3 | 0 | 5 | 283 | 0 | 0 | 0 | 0 | 0 |
| 4 | 0 | 0 | 0 | 288 | 0 | 0 | 0 | 0 |
| 5 | 0 | 0 | 0 | 0 | 288 | 0 | 0 | 0 |
| 6 | 0 | 0 | 0 | 0 | 0 | 288 | 0 | 0 |
| 7 | 0 | 0 | 0 | 0 | 0 | 0 | 288 | 0 |
| 8 | 10 | 0 | 0 | 0 | 0 | 0 | 0 | 278 |

Table 3: Confusion matrix of Algorithm A, that uses spatial image features, on the test set.

| | Given Class | | | | | | | |
|---|---|---|---|---|---|---|---|---|
| | 1 | 2 | 3 | 4 | 5 | 6 | 7 | 8 |
| Desired Class | | | | | | | | |
| 1 | 247 | 0 | 7 | 6 | 0 | 5 | 1 | 22 |
| 2 | 1 | 245 | 28 | 2 | 0 | 3 | 9 | 0 |
| 3 | 4 | 20 | 234 | 0 | 0 | 12 | 14 | 4 |
| 4 | 1 | 3 | 0 | 284 | 0 | 0 | 0 | 0 |
| 5 | 0 | 0 | 0 | 0 | 285 | 2 | 1 | 0 |
| 6 | 1 | 2 | 6 | 0 | 2 | 271 | 4 | 2 |
| 7 | 1 | 21 | 6 | 0 | 11 | 3 | 246 | 0 |
| 8 | 22 | 0 | 2 | 0 | 0 | 5 | 1 | 258 |

Table 4: Confusion matrix of Algorithm B, that employs range profiles, on the test set.

| | Given Class | | | | | | | |
|---|---|---|---|---|---|---|---|---|
| | 1 | 2 | 3 | 4 | 5 | 6 | 7 | 8 |
| Desired Class | | | | | | | | |
| 1 | 253 | 0 | 5 | 5 | 0 | 8 | 1 | 16 |
| 2 | 2 | 259 | 18 | 1 | 0 | 6 | 2 | 0 |
| 3 | 4 | 12 | 259 | 0 | 0 | 9 | 4 | 0 |
| 4 | 0 | 0 | 1 | 286 | 0 | 0 | 1 | 0 |
| 5 | 0 | 0 | 0 | 0 | 282 | 4 | 2 | 0 |
| 6 | 3 | 0 | 3 | 0 | 0 | 264 | 17 | 1 |
| 7 | 0 | 9 | 8 | 0 | 3 | 9 | 259 | 0 |
| 8 | 31 | 0 | 2 | 0 | 0 | 1 | 1 | 253 |

Table 5: Confusion matrix of Algorithm C, that uses de-speckled range profiles, on the test set.

Next, the tradeoff between computational complexity and performance was examined. A similar experimental setup was used which incorporated training, validation and test data sets as described previously, except that the aspect angle range included 49 views in the [30,150] degree range, in 2.5 degree increments. First, the effect of the number of input nodes on performance were examined; the input nodes for the square-block features were set at 81, 9x9 pixel blocks, making the number of input nodes comparable to that of the number of range profile features. From Table 6, it can be seen that the performance degradation from 256 to 81 inputs is small.

Improvement using a multi-resolution representation is also shown in Table 6 where 50 and 75 nodes corresponding to two and three resolution levels were tested. For the 50 input case, 25 16x16 pixel block features were used for low resolution while 25 5x5 centered pixel blocks were used at high resolution. For the 75 input case, an intermediate resolution of 25 10x10 pixel block input nodes were added. Also shown in Table 6 are the approximate training and validation CPU running times, indicating decreased training time with increased performance.

# 4 CONCLUSION

This paper has demonstrated the viability of utilizing BP neural networks in classifying ship targets found in airborne SAR imagery. A correct classification rate as high as 98% has been obtained. Three different algorithms for feature extraction have been applied and compared. Back-propagation classifiers that utilize the entire SAR image as input significantly outperform classifiers that utilize

| # Inputs | Pixel Block Size | # Hidden Layers | % Correct | Training Time |
|---|---|---|---|---|
| 256 | 5x5 | 10 | 99.3 | 3 hrs |
| 81 | 9x9 | 19 | 98.1 | 6 hrs |
| 50 | 16x16<br>5x5 | 13 | 97.6 | 4 hrs |
| 75 | 16x16<br>10x10<br>5x5 | 15 | 98.5 | 2 hrs |

Table 6: Performance and complexity of pixel block feature BP network as a function of the number of input nodes and number of resolutions.

range profiles. It is also shown that although speckle reduction pre-processing prior to range profiling improves the performance of BP classifiers, the improvement was not that significant. Finally, it was demonstrated that multi-resolution pixel block features were able to provide improved performance at reduced processing.

# 5 ACKNOWLEDGMENTS

This work was performed while the first author was a Research Scientist and NSERC Postdoctoral Fellow at Queen's University. The authors would like to acknowledge the support given in part by Lockheed Martin Electronic Systems, Montreal, Quebec, and in part by the Natural Science and Engineering Research Council (NSERC) of Canada under grant no. CRD 177119.

# 6 REFERENCES


1. H. Osman and Steven D. Blostein,"SAR image processing using probabilistic winner-take-all learning and artificial neural networks," in *Proceedings of the IEEE International Conference on Image Processing (ICIP)*, vol. II, pp. 613-616, Lausanne Switzerland, 1996.

2. H. Osman and Steven D. Blostein, "SAR imagery segmentation using probabilistic winner-take-all clustering," in *Proceedings of SPIE Conference on Algorithms for Synthetic Aperture Radar Imagery III*, vol. 2757, pp. 217-226, Orlando USA, 1996.

3. K. Eldhuset, "An automatic ship and ship wake detection system for spaceborne SAR images in coastal regions," IEEE Transactions on Geoscience and Remote Sensing, vol. 34, no. 4, pp. 1010-1019, 1996.

4. G. Benelli, A. Garzelli, and A. Mecocci, "Complete processing system that uses fuzzy logic for ship detection in SAR images," IEE Proc.-Radar, Sonar Navig., vol. 141, no. 4, pp. 181-186, 1994.

5. M. Rey, J.K.E. Tunaley, and T. Sibbald, "Use of the Dempster-Shafer algorithm for the detection of SAR ship wakes," IEEE Transactions on Geoscience and Remote Sensing, vol. 31, no. 5, pp. 1114-1118, 1993.

6. M. Rey, J.K.E. Tunaley, J.T. Folinsbee, P.A. Jahans, J.A. Dixon, and M.R. Vant, "Application of radon transform techniques to wake detection in Seasat-A SAR images," IEEE Transactions on Geoscience and Remote Sensing, vol. 28, no. 4, pp. 553-560, 1990.

7. "RIG, The Radar Imagery Simulator," Version 3.0, Technology Service Corporation, 1996.

8. Jong-Sen Lee, "Speckle analysis and smoothing of synthetic aperture radar images," Computer Graphics and Image Processing, vol. 17, pp. 24-32, 1981.